https://doi.org/10.5194/egusphere-2026-3253
Preprint. Discussion started: 24 June 2026

Mechanistic modeling of the impact of rainfall pumping on soil solute remobilization into runoff

Lucie Guertault[1], Rafael Muñoz-Carpena[2]

[1]Department of Biological and Agricultural Engineering, North Carolina State University, Raleigh, NC 27695, USA
[2]Department of Agricultural and Biological Engineering, University of Florida, Gainesville, FL 32611, USA

Correspondence to: Lucie Guertault (lsguerta@ncsu.dedu)

Abstract. The remobilization of solutes from the soil to surface runoff is a critical process for surface water contamination, yet it remains challenging to model mechanistically. This study explores a novel mechanistic modeling approach that explicitly accounts for local advective transport driven by pressure fluctuations induced by raindrop impacts ("rainfall pumping") on the soil surface. We coupled the HYDRUS-1D model with a time variable, surface pressure head boundary condition, which combines runoff depth and the semi empirical, sinusoidal rainfall pumping wave of Higashino and Stefan (2014) whose amplitude and frequency are estimated from runoff depth and rainfall intensity. This boundary condition was tested for the first time against experimental data on saturated soils using two benchmark studies: one for model development and another for independent verification. Two additional datasets were used to verify the physical consistency of the pressure head values estimated by the pumping formulation. The results were compared with those from a conventional "no-pumping", fixed runoff depth boundary condition. The rainfall-pumping boundary condition improved estimates of the final soil bromide concentration profile, solute extraction depth, and total remobilized mass, with the pumping model achieving the best predictions across all soils (final concentration profile NSE = 0.997, 0.977, 0.620, 0.881 for the sandy loam, loam and clay soils in the development phase and the loamy soil the verification phase, respectively). The results support the importance of accounting for the physical rainfall pumping process to explain enhanced solute extraction from soils during storms and to avoid unrealistic transport parametrization.

1 Introduction

Excess chemicals stored in the soil near the surface are susceptible to being remobilized into runoff during rainfall-runoff events, causing downslope contamination of surface water bodies. The prediction of chemical remobilization from soils into runoff is critical for many applications, such as the regulatory risk assessment and management of agrochemicals. Previous studies have established limited qualitative relationships between the chemical concentrations in runoff and individual environmental factors including soil hydraulic properties (Ahuja and Lehman, 1983; Havis et al., 1992; Snyder and Woolhiser, 1985), infiltration rates (Ahuja and Lehman, 1983), rainfall intensity (Snyder and Woolhiser, 1985; Thompson et al., 2010; Wang et al., 2002; Zhang et al., 2020), and surface slope (Deng et al., 2019). Experimental data from Havis et al.

https://doi.org/10.5194/egusphere-2026-3253
Preprint. Discussion started: 24 June 2026

(1992) also showed distinct chemical remobilization patterns from soil to runoff across soil types and rainfall intensities, suggesting complex interactions between the processes at play.

To this date, Ahuja and Lehman (1983) and Havis (1986) experiments remain the most complete experiments on solute remobilization from soil to runoff. Ahuja and Lehman (1983) performed experiments on three distinct soils identified as sandy loam, loam and clay, and tested one rainfall rate (68 mm h^{-1}) with three bottom flow conditions: impervious base (no infiltration), free bottom drainage, and slurry base (intermediate infiltration rate). Their observations include the solute concentration profile in the soil at the end of the experiments as well as the solute concentration in runoff over time. As a result, this experimental data has been widely used to test various models simulating the remobilization of chemicals from the soil to the runoff (Wallach et al., 1988; Walter et al., 2007). Havis (1986) also performed experiments with impervious base on loamy soil with rainfall rates ranging from 60 to 163 mm $h^{-1}$and reported final concentration profiles in the soil.

The first modeling approaches developed for predicting the surface runoff remobilization of soil chemicals date back to the 1970s (Bruce et al., 1975). These models were based on the conceptual assumption that there is a thin surface layer of soil of fixed thickness where the concentration is uniform, called the “soil mixing layer”, which partially mixes with runoff with a constant degree of mixing. However, the experimental data provided by Ahuja and Lehman (1983) showed that the removal of solutes from soils is not uniform with depth and varies across soils, thus contradicting the empirical assumption of a fixed uniform soil mixing layer. To refine the mixing layer approach, several authors introduced non-uniform mixing layer models. For example, Young and Fry (2017) proposed that the fraction of pore water interacting with the runoff decreases with depth. Shao et al. (2021) proposed an alternative where the thickness of the mixing layer varies with time. In these models, the thickness of the mixing layer and interacting fractions are fixed empirically independently of soil, rainfall and runoff characteristics, or are calibrated to match observations. The mixing layer modeling approach remains limited by a heavy reliance on empirical parameterization rather than a mechanistic description of the processes of chemical removal.

Alternative modeling approaches have also been proposed that do not rely on a “mixing layer” but instead introduce empirical modifications to the chemical diffusion transport at the surface of the soil (Havis et al., 1992; Parr et al., 1987; Wallach et al., 1988; Wallach and Shabtai, 1993). They are based on the observation that when soil infiltration is suppressed, molecular diffusion alone is not sufficient to explain the observed magnitude of the chemical fluxes from the soil to the runoff, especially at the beginning of the remobilization process (Figure 1b). For example, Wallach et al. (1988), proposed a model applicable for scenarios when infiltration is suppressed, for example when there is no bottom flux and the soil is saturated. They relied on the theory that a boundary layer exists at the interface between the soil and the runoff, which enhances the mass transfer from areas of high chemical concentration (typically the soil) to areas of low chemical concentration (typically the overlying runoff). For this the authors introduced an effective mass transfer coefficient derived from the boundary layer theory for laminar flow over a flat uniform plate. The effective mass transfer coefficient depended on the molecular diffusion coefficient of the chemical, fluid viscosity, runoff velocity and depth, and the length of the slope. Wallach et al. (1988) tested their model against the data from Ahuja and Lehman (1983) experiments with no infiltration and one of the soils (loam) and reported that the model reproduced well the experimental observations. We evaluated

https://doi.org/10.5194/egusphere-2026-3253
Preprint. Discussion started: 24 June 2026

preliminarily the Wallach et al. (1988) model performance by calculating the Nash Sutcliffe Efficiency (NSE) with the null hypothesis threshold Ho:NSE < 0.65 (Ritter and Muñoz-Carpena, 2013), and found that their proposed model did not pass the statistical test (p-value=0.16, results not shown). This indicates that the uniform flat plate approximation is likely inappropriate for soils, which are heterogenous media with a rough surface.

The mismatch between the experimental data and outputs from current modeling approaches suggests that a more robust, mechanistic approach is required. To bridge this gap, recent research has pivoted toward simulating the advective transport processes that can enhance transport of contaminants from the soil to the runoff, like rainfall pumping. Rainfall pumping refers to the pressure fluctuations generated at the soil-water interface during raindrop impact that drive upward and downward flow in a thin layer of soil below the surface. Experimental data suggest that in the presence of a thin layer of water, typical rainfall pumping can result in pressure heads at the soil surface up to 30 cm (Palmer, 1965; Yu and Hopkins, 2018). This process can drive the exchange of pore water and chemicals, providing a physical explanation for the enhanced remobilization observed in laboratory experiments.

Higashino and Stefan (2014) proposed a semi-empirical formula to quantify the pressure at the soil surface caused by "rainfall pumping" (Figure 1a), where the pressure amplitude is inversely proportional to the runoff depth. Assuming saturated media, they proposed that the magnitude of interfacial water fluxes can range (after the correction introduced later in this manuscript) from 10^{-4} to 1 cm s^{-1}. However, the validity of this formulation has not been ascertained by testing against experimental data.

We posit here that a mechanistic model that reflects the actual advective and dispersive transport processes at the soil-runoff interface by coupling explicit soil flow and transport equations with a boundary condition quantifying the rainfall pumping surface pressure fluctuations can effectively and consistently predict the solute tracer remobilization profile, mass and depth of solute extraction (Figure 1b).

https://doi.org/10.5194/egusphere-2026-3253
Preprint. Discussion started: 24 June 2026

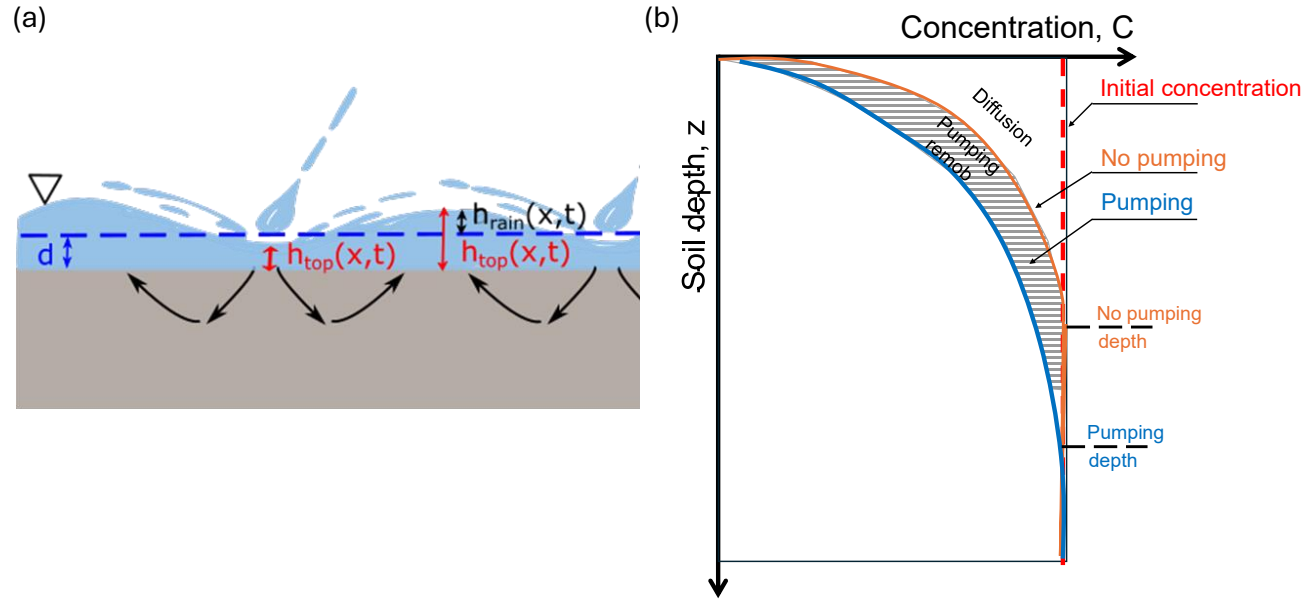

Figure 1. (a) Representation of the variable pressure head at the top of the soil with rainfall pumping, (b) impact of rainfall pumping on solute extraction from the soil and depth of removal after the event. The area above each of the curves (diffusion and pumping) represents the mass remobilized by each process, where the mass with pumping is larger.

Thus, the objectives of this study are to i) develop a modeling approach for the remobilization of soil chemicals that couples flow and transport processes in the soil with Higashino and Stefan (2014) top boundary condition to represent pressure fluctuations generated by the rainfall pumping processes; ii) validate the approach against the experimental data from Ahuja and Lehman (1983) and Havis (1986) and physically realistic rain pumping pressure values (Palmer, 1965; Yu and Hopkins, 2018); and iii) compare the approach with the classical "diffusion" (no-pumping) boundary condition approach.

2 Methods

2.1 Experimental data

An extensive literature review found only two experimental rainfall-runoff soil solute removal datasets where the inputs needed to test the proposed mechanistic rainfall pumping approach were available. The Ahuja and Lehman (1983) experiments were used for the initial model testing while the Havis (1986) experiments were used for independent model verification. These impervious base experiments were selected because they eliminate the downward infiltration process and clearly isolate the near surface soil processes responsible for the solute remobilization and transfer to runoff. In Ahuja and Lehman (1983) experiments, soil boxes 1.0 m long, 0.15 m wide and 0.10 m deep with no bottom drainage were filled with soil and saturated with a bromide solution at an approximate target concentration of 0.004 g cm^{-3}. Three distinct soils identified as sandy loam, loam and clay were used, with bulk densities of 1.35, 1.42 and 1.21 g cm^{-3}, respectively and

https://doi.org/10.5194/egusphere-2026-3253
Preprint. Discussion started: 24 June 2026

corresponding saturated volumetric water contents of θ_s =0.53, 0.49 and 0.55. The saturated hydraulic conductivities were estimated to be $K_s \approx$ 2.75 cm h^{-1} (7.64x10^{-4} cm s^{-1}), 1.39 cm h^{-1} (3.89 x10^{-4} cm s^{-1}), and 1.58 cm h^{-1} (4.39 x10^{-4} cm s^{-1}). Ahuja and Lehman (1983) reported that some swelling of the clay occurred during the experiments that increased the saturated hydraulic conductivity. Rainfall runoff experiments were conducted with a rainfall intensity of 68 mm h^{-1} for a duration of 61 minutes. The rain simulator placed 2.5 m over the soil produced drops of 3.0 mm. The concentration of bromide in the runoff was measured at the start of the runoff and after 5, 10, 20, 30, 40, 50 and 60 minutes. At the end of the experiment, bromide concentrations in the soil were measured at approximate depths of 0.12, 0.25, 0.75, 1.5, 2.5, 3.5 and 4.5 cm. Each experiment was replicated four times. Some variability was observed in the soil solute concentration data between replicated experiments. In addition, for the clay and loamy soils, the final concentrations at depths below 2.5 cm, where no solute remobilization is expected, exceeded the initial concentration value reported of 0.004 g cm^{-3}, suggesting that the initial concentrations were slightly larger than reported and might not be uniform.

In Havis (1986) experiments, a loamy soil was placed in a 15 cm diameter and 15 cm tall cylinder. The soil was packed with a density of 1.1 g cm^{-3} and equivalent porosity of $\theta \approx 0.58$. The soil was saturated with a bromide solution at a target concentration of 0.004 g cm^{-3}. This experiment was conducted with a rainfall intensity of 150 mm h^{-1} for 30 minutes. The rainfall simulator used generated drops with a 3.2 mm diameter falling from a height of 7.9 m. At the end of the experiment, the soil was sampled at depths from 0 to 4.5 cm to determine the solute concentration in the profile.

To evaluate the physical validity of the proposed pumping boundary condition, empirical data quantifying the pressure caused by raindrop impact on ponded surfaces was gathered from the literature for comparison with the simulated pressure values. Palmer (1965) used a strain gage to estimate the strain caused by water drops of diameters of 2.9, 4.7, and 5.9 mm impacting a rubber membrane from a height of 1.5 m with layers of water ranging from 0 to 30 mm. They converted the strain into a stress value using a strain-stress calibration curve. Yu and Hopkins (2018) recorded time-dependent impact forces for water drops of 2 and 4.5 mm diameters falling at various velocities and impacting a glass plate with layers of water ranging from 0 to 10 mm. In both cases, we converted experimental forces to average pressure head to facilitate a direct comparison with the boundary condition estimates. We created a response surface graph for each dataset and the experimental conditions of Ahuja and Lehman (1983) and Havis (1986) were overlaid on the graphs to extract representative raindrop pressure values for these experiments and compare them with the simulated values.

2.2 Model description

The proposed mechanistic approach couples Hydrus 1D (Šimůnek et al., 2008) for the simulation of flow and transport in a one-dimensional soil profile with the physical boundary condition representing the dynamic rainfall pumping pressure at the top of the soil. Hydrus 1D is a simulation software that numerically solves Richards Equation for saturated-unsaturated water flow coupled with the advection dispersion equation for solute transport using a finite element method. It offers several soil hydraulic parameters models, including the van Genuchten - Mualen model (van Genuchten, 1980), which was used in this study. It also contains several boundary condition types to accommodate real-world scenarios.

https://doi.org/10.5194/egusphere-2026-3253
Preprint. Discussion started: 24 June 2026

In this study, rainfall pumping is introduced as a time variable pressure head top boundary condition in Hydrus 1D (read from an external file). The pressure head function at the top of the soil h_{top} (m) is represented as the sum of the runoff depth d (m) and a sinusoidal term quantifying the variable pressure caused by raindrop impact proposed by Higashino and Stefan (2014) (Figure 1a) as:

$$h_{top,p} = d + h_0 \sin(\omega_h t) \quad (1)$$

where h_0 (m) is the amplitude, or maximum pressure caused by the impact, and ω_h is the frequency, interpreted as the frequency between two raindrop impacts at the same location. Assuming that the kinetic energy of the raindrops is transformed into pressure when they reach the ground, Higashino and Stefan (2014) proposed the following relationship for h_0,

$$h_0 = \frac{W_2 \, V^2}{2gd} \quad (2)$$

where W_2 is the volume of raindrops reaching a unit surface (m), V is the terminal velocity of the raindrops (m s^{-1}), g is the acceleration of gravity (m s^{-2}), d (m) is the runoff depth.

Higashino and Stefan (2014) also proposed empirical relationships for W_2 (mm^3 m^{-2} s^{-1})), V (m s^{-1}) and ω_h (s^{-1}) as functions of the rainfall intensity R (mm h^{-1}),

$$W_2 = 7.12R^{0.77} \quad (3)$$

$$V = 9.65 - \frac{22457.8}{(R^{0.21} + 6.83333)^4} \quad (4)$$

$$\omega_h = \frac{2\pi \, R^{0.23}}{0.0256} \quad (5)$$

Note that Eq. 2 and 3 are taken directly from Higashino and Stefan (2014), but that the dimension of W_2 differs in the two equations. Equations 2-5 indicate that $h_{top,p}$ depends on the runoff depth and rainfall intensity, and that the amplitude of the dynamic pumping pressure h_o is proposed to be inversely related to the effective runoff depth. We performed a careful review of Higashino and Stefan (2014) Eq. (3) for W_2 and found that as originally presented it provides unrealistic values. For example, for the rainfall rate of 68 mm h^{-1} used in Ahuja and Lehman (1983) experiments, Eq. 3 gives a volume of raindrops reaching a unit surface of 183 mm^3 m^{-2} s^{-1}. However, 68 mm h^{-1}=68 L m^{-2} h^{-1} means 68,000,000 mm^3 of rain falls over 1 m^2 in an hour, so approximately 18,900 mm^3 m^{-2} s^{-1}. As a result, the original Higashino formulation underestimates W_2 by a factor of ~100 and leads to wrong estimates of h_0 and ω_h. Therefore, we corrected the equations for W_2 and ω_h in this study as,

$$W_2 = 712R^{0.77} \quad (6)$$

$$\omega_h = \frac{2\pi \, R^{0.23}}{2.56} \quad (7)$$

https://doi.org/10.5194/egusphere-2026-3253
Preprint. Discussion started: 24 June 2026

For comparison, the "classical" (no-pumping) boundary condition was also tested in Hydrus 1D. It considers solute diffusion from the surface assuming surface pressure equal to the runoff depth during the experiment and neglecting the pressure caused by raindrops as:

$$h_{top,np} = d \tag{8}$$

2.3 Model testing and verification

The evaluation of the proposed rainfall pumping boundary condition was conducted through a three-phase modeling framework designed to identify model parameters for the experimental system, compare the proposed pumping boundary condition over the classical no-pumping boundary condition, and validate the model's transferability across different experimental datasets.

2.3.1 Model application for Ahuja and Lehman experiments

Three modeling scenarios were developed to test the impact of the pumping boundary condition on solute removal. The first modeling scenario consisted of identifying optimal soil hydraulic and transport parameters for the no-pumping boundary condition (Eq. 8) (np_c scenario), representing classical modeling approaches. The second scenario consisted of identifying optimal soil hydraulic and transport parameters for the pumping boundary condition (Eq. 1) (p_h scenario). The third scenario (np_h) combined the no-pumping boundary condition with parameters from the p_h scenario to evaluate the direct impact of the pumping boundary condition on solute removal.

The 3 scenarios were applied to each of the Ahuja and Lehman soil datasets for sandy loam, loam and clay. The tests were designated by the soil prefix (SL, L, C for sandy loam, loam and clay), followed by the modeling scenarios suffix (np_c, p_h, np_h).

The HYDRUS 1D computational domain consisted of a 10-cm deep vertical soil profile with a 0.2-cm finite element mesh. For all tests, the diffusion coefficient for bromide was set to its standard molecular diffusion 1.85×10^{-5} cm^2 s^{-1} (Haynes, 2016). In the simulations, the initial condition was a saturated soil with uniform solute concentration of bromide. For each soil this initial concentration was set equal to the average of measured concentrations below the area of solute extraction (2.5, 3.5 and 4.5 cm) at the end of the experiments. It corresponded to 0.00356 g cm^{-3}, 0.00478 g cm^{-3} and 0.00440 g cm^{-3} for the SL, L and C soils, respectively. The bottom boundary condition was set to zero flux to represent the impervious base. For solute transport, the top boundary condition set equal to the runoff bromide concentration. In the experimental data presented by Ahuja and Lehman (1983), within five minutes of the start of the test the Br concentrations in runoff were ~0 (<10^{-4}) g cm^{-3} so the top boundary condition was set to zero. This approach may slightly overestimate the dispersion fluxes at the soil runoff interface for the first minutes of the simulation but closely matched the conditions of the rest of the experiment.

For the np_c scenario, the optimization algorithm in Hydrus 1D was used to obtain the soil hydraulic parameters and dispersivity. For the p_h scenario, given the limited information on the soils provided in Ahuja and Lehman (1983), the

https://doi.org/10.5194/egusphere-2026-3253
Preprint. Discussion started: 24 June 2026

search range (Table 1) for the van Genuchten's (vG) soil hydraulic parameters was selected based on the ranges for all the soil textures provided by Meyer and Taira (2001). The range for soil dispersivity (λ) was based on the ranges provided by Beven et al. (1993) from soil cores. The initial input estimates were set to default values for the soil texture found in the Hydrus 1D software soil catalog and the initial estimate of dispersivity was set to 200 cm (Table 1). The runoff depth (d) was set to 0.07 cm as estimated by Wallach et al. (1988) for these experiments using open channel flow equations.

For the _p_h scenario, a global search method with local refinement similar to that of Luquin et al. (2021) was employed to identify the effective soil, transport and runoff parameters for each soil experiment by generating a set of input combinations that systematically sampled the hyperdimensional input space with specified search ranges. Sobol (1993) numerical sequences were used to sample the input sets for the global search as they provide an efficient and robust distribution across the high-dimensional input space (Saltelli et al., 2008). The number of simulations required is $N=M\ (k+2)$ for each case, where k is the number of input factors (k=6) and M is the oversampling rate selected here as 2048 (N=16384). For each input combination, the pumping boundary condition was calculated and the model was run. The Nash and Sutcliffe (1970) model coefficient of efficiency (NSE) was calculated for the paired observed and predicted final Br soil concentration values at various depth. After all the simulations were completed, the results were ranked from high to low NSE values to select the effective input set for each soil. The model simulations were performed in parallel at the University of Florida high performance computer, HiperGator, using R scripts and 'wine' (windows emulator under linux) to automate the input and boundary condition substitutions in Hydrus-1D files, executing the program, and calculating NSE against observations.

The third scenario (np_h) combined the no-pumping boundary condition (Eq. 8) with the model parameters identified for the p_h case.

Table 1. Model parameters and range used for the global search optimization and initial values used in the Hydrus 1D optimization algorithm

Input	Initial value for np_c		Search range for p_h	Sources
	Clay	Loam	Clay	
vG θ_r ($cm^3\ cm^{-3}$)	0.068	0.078	0.068	0.00087 -0.14	Meyer and Taira (2001)
vG α (cm^{-1})	0.008	0.036	0.008	0.0003 - 0.202	Meyer and Taira (2001)
vG n (-)	1.09	1.56	1.09	0.80 - 2.43	Meyer and Taira (2001)
vG K_{sat} ($cm\ s^{-1}$)	$5.5x10^{-5}$	$2.9x10^{-4}$	$5.5x10^{-5}$	$1.7x10^{-5}$ - $3.5x10^{-2}$	Meyer and Taira (2001)
λ (cm)	200	200	200	10 - 1000	Beven et al.(1993)
d (cm)	0.07	0.07	0.07	0.0025 - 4 *	Wallach et al. (1988)

* d not optimized in the np_c scenario

https://doi.org/10.5194/egusphere-2026-3253
Preprint. Discussion started: 24 June 2026

To determine if the differences in modeled soil concentrations between the pumping and no-pumping scenarios (p_h vs np_h) are statistically significant or if they were just artifacts of the uncertainties on the initial soil concentration, a separate uncertainty analysis was performed whereby the uncertainty of initial condition was propagated through the np_h simulation results. For each soil, N'=1208 alternative initial Br soil concentrations were generated, with values ranging from the minimum (0.0038, 0.0037, 0.0030 for C, L, SL respectively) to the maximum (0.0047, 0.0049, 0.0042 for C, L, SL respectively) of experimental values reported at depths below 2.5 cm. The model was run for each initial concentration value, and the ensemble results were used to calculate the confidence intervals for the simulated Bromide profiles in the np_h scenario. This set of simulations was compared with the observation ranges and the outputs from the p_h simulations to identify if these were sufficiently separated (non-overlapping) to attribute the differences to the boundary conditions instead of the experimental uncertainty.

2.3.2 Independent model verification

To verify the model independently, the robustness and impact of the pumping boundary condition on contaminant removal were evaluated using Havis (1986) loamy soil dataset. The loamy soil parameters previously identified for Ahuja and Lehman experiments with the pumping boundary condition (L_p_h scenario) were reused to simulate the Havis experiments without further adjustment using the pumping (HL_p_h) and no-pumping boundary conditions (HL_np_h). This step aimed to verify if the pumping boundary condition could maintain superior accuracy over the classical no-pumping boundary condition across different experimental setups thereby validating the proposed mechanistic boundary condition.

2.3.3 Model evaluation

For all modeling scenarios, the model goodness of fit was evaluated with the FITEVAL software (Ritter and Muñoz-Carpena, 2013). For a given array of observed and predicted values, FITEVAL calculates the goodness of fit/prediction measures NSE (Nash and Sutcliffe, 1970), Kling-Gupta Efficiency (KGE; Gupta et al., 2009) and root mean square error (RMSE), detection of outliers, and model bias. FITEVAL provides an objective statistical hypothesis testing framework for model adequacy based on the significance (p-value) of the model performance below a desirable minimum efficiency threshold Ho: NSE < 0.65 (Ritter and Muñoz-Carpena, 2013) or NSE < 0.50 (Moriasi et al., 2007). In addition, model performance pedigrees are assigned by these authors based on the test as "unacceptable" (NSE <0.65), "acceptable" (0.65≤NSE<0.8), "good" (0.8≤NSE<0.9) and "very good" (NSE≥0.9).

2.4 Mass of solute extracted and depth of removal

For each experiment and simulation with the alternative boundary conditions, the mass of solute extracted ($M_{s,ext}$) from the soil was calculated based on the initial and final solute concentration profiles in the soil,

$$M_{s,ext} = A.\theta_s\left(C_o.z_t - \int_o^{z_t} C(z)dz\right) \quad (16)$$

https://doi.org/10.5194/egusphere-2026-3253
Preprint. Discussion started: 24 June 2026

where A (cm^2) is the surface area of the soil box, θ_s is the saturated water content, C_o is the initial uniform bromide concentration (g cm^{-3}), z_t (cm) is the depth of the soil profile, $C(z)$ is the bromide concentration in the soil with depth (z) at the end of the experiment (g cm^{-3}). The integral was solved numerically with a Gauss quadrature of order 4 based on the experimental or numerical results.

The depth of solute removal was estimated as the depth at which the final solute concentration is equal to the initial concentration. For Ahuja and Lehman dataset, only seven experimental data points were available and, as variability was observed in the concentrations at deeper locations in the soil, the approximate depth of solute removal was estimated by exponential interpolation the observations across locations in the soil.

2.5 Analysis of input factor importance

Global sensitivity analysis (GSA) (Saltelli, 2002) was employed in the p_h scenario to study the pumping boundary condition input factors controlling the Br mass extracted from the soil for the Ahuja and Lehman simulations. By varying concurrently all input factors within their validity domain defined by probability distribution functions, GSA allows for simultaneous estimation of the system input factors' individual importance (direct or first order effects) and interactions (higher order effects) (Lauvernet and Muñoz-Carpena, 2018; Saltelli et al., 2005). We employed the Sobol (1993) variance-decomposition method as it has proven superior for irregular outputs making it suitable for difficult problems (Saltelli et al., 2005). In GSA variance-decomposition, the total model output variance is decomposed in fractions attributed to each input factor's direct effects (first-order sensitivity index, S_i) or with factor interactions (total sensitivity index, S_{Ti}) (Saltelli et al., 2005; Sobol, 1993). Interactions for each input can be estimated as the difference between the total and first order indices, S_{Ti} - S_i. In the case of a purely additive model, i.e. a model without interactions between inputs, $\Sigma_i S_i = \Sigma_i S_{Ti} = 1$, otherwise, $\Sigma_i S_i < 1$ and $\Sigma_i S_{Ti} > 1$. For practical purposes, a model is considered "mostly additive" when $\Sigma_i S_i \leq 0.6$ (Saltelli, 2004). The Sobol's GSA was performed with the SALib python package using the function *saltelli* (Herman and Usher, 2017), with uniform distributions corresponding to the search ranges in Table 1.

3. Results

3.1 Comparison of model performance

For Ahuja and Lehman experiments, the best performance was achieved by the pumping boundary condition (p_h), with NSE values of 0.621, 0.977, 0.997 (Table 2) for the clay, loam and sandy loam, respectively. For the clay and loamy soils, the no-pumping boundary conditions perform worse with NSE dropping to 0.438 and 0.886, respectively.

For the clay soil, all modeling scenarios p-values showed that the null hypothesis of unacceptable model (NSE<0.50) could not be rejected. C_p_h has a p–value=0.2, which is much smaller than the other scenarios. However, the visual assessment of the final solute concentration profiles in the soil (Figure 2) reveals that the modeled final concentration profile for C_p_h fits the observation data best, particularly in the top of the soil where mass is extracted. The simulated profile falls within the

https://doi.org/10.5194/egusphere-2026-3253
Preprint. Discussion started: 24 June 2026

observed data error bounds, except at depth -0.25 cm. No-pumping scenarios C_np_h and C_np_c largely overestimate the concentration compared to the experimental data at depth -0.75 cm, even when accounting for the propagation of the uncertainty on the initial soil concentration value in the no-pumping modeling scenario C_np_h. The C_p_h scenario exhibits a distinct soil solute removal and redistribution pattern where the front of solute removal is less sharp (less horizontal) and reaches deeper compared to the no-pumping conditions. This indicates that the improvement that is observed for C_p_h can be attributed to the pumping boundary condition as proposed earlier in Fig. 1b.

For the loamy soil, all scenarios passed the significance test, rejecting the null hypothesis NSE<0.50, but only the pumping scenario L_p_h passed the significance test for the stricter NSE< 0.65. Visually, the final concentration profile for L_p_h is the only scenario that matches observations, and the no-pumping scenarios overestimate the concentration (Figure 2). For the sandy loam soil, all scenarios displayed NSE above 0.90 and passed the significance test, rejecting the hypothesis that NSE< 0.65. However, the visual assessment of the final concentration profiles in the sandy loam soil at the end of the event reveals that the Hydrus 1D classical condition (SL_np_c) does not match the observations in the extraction zone (depths of -0.25 cm and -0.75 cm), while the others do (Figure 3). The improvement in model performance with the addition of the pumping boundary condition (between SL_np_h and SL_p_h) is only marginal with both producing very good results, while the improvement in model performance between SL_np_c and SL_np_h is more significant.

For the Havis (1986) loamy soil experiment, the pumping boundary condition (HL_p_h) provided very good results (NSE=0.881) and passed the significance test for NSE <0.65. The non-pumping boundary condition resulted in a poor NSE = 0.077, with p-values well above the significance level for NSE <0.50. This independent dataset supports that the addition of the pumping boundary condition significantly improves the model outputs without calibration of the soil and transport parameters. Visually, the final concentration profile in the HL_p_h simulation matched the observations closely, except for two points around the depth of – 1 cm. These two points seem experimental outliers as other points at similar depths showed lower concentrations matching the simulations. The HL_np_h simulation overestimated the concentration profile in the top 2 cm of the soil profile.

https://doi.org/10.5194/egusphere-2026-3253
Preprint. Discussion started: 24 June 2026

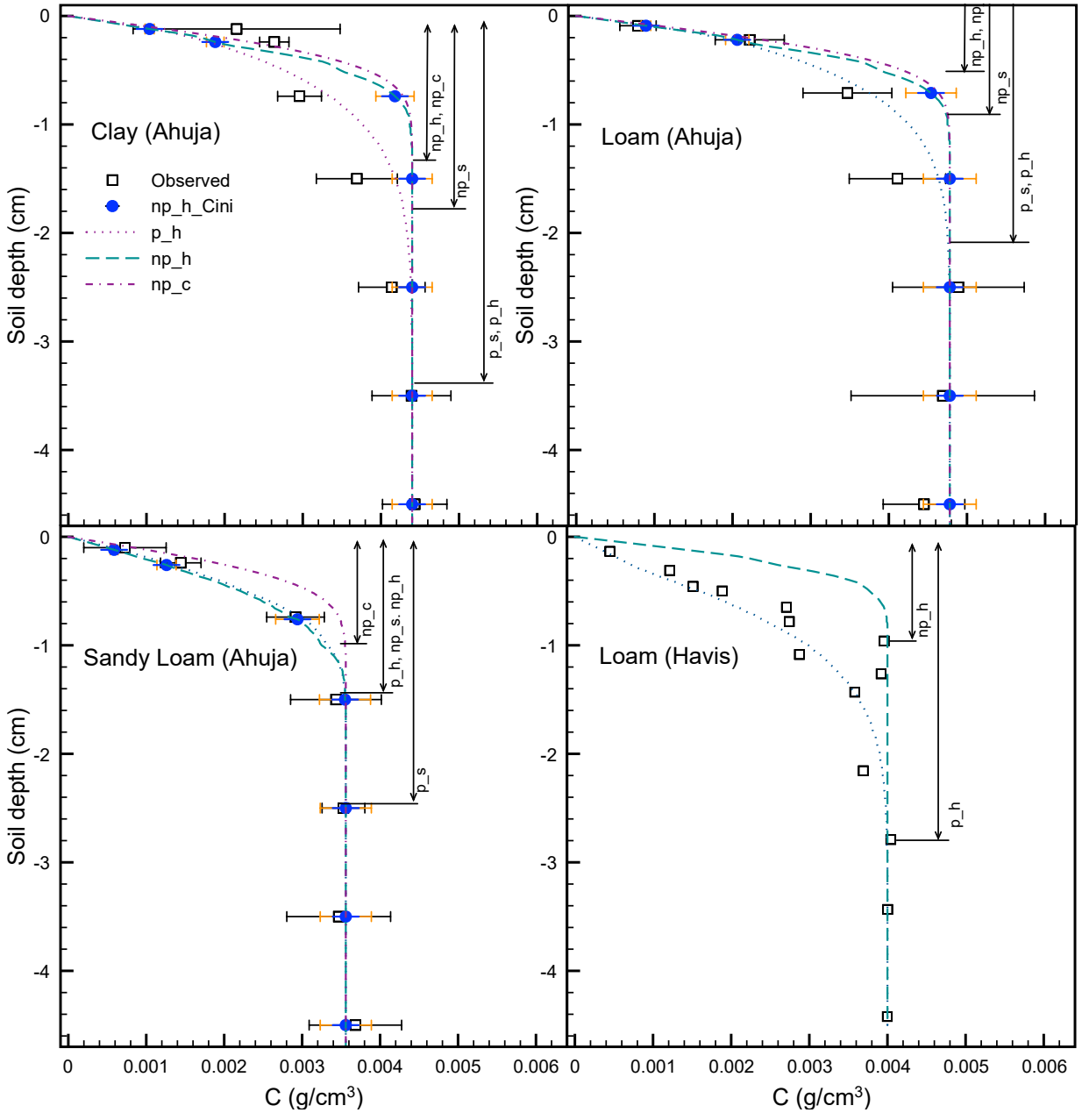

Figure 2. Comparison of simulation results against experimental data (Ahuja and Lehman, 1983, Havis, 1986). Symbols for cases are: C, L, SL: Ahuja and Lehman clay loam and sandy loam soils; HL: Havis's loamy soil, p_h is for the optimized soil and transport parameters with Higashino-pumping boundary condition, np_h uses the same soil and transport parameters with no-pumping, np_c is the Hydrus 1-D no-pumping with optimization algorithm. Error bars on observation data show standard deviation of observed values (n=4). Error bars on the np_h model outputs show the standard deviation of the output when varying the initial concentration in the soil profile.

https://doi.org/10.5194/egusphere-2026-3253
Preprint. Discussion started: 24 June 2026

Table 2. Model testing against concentration (C, g cm^{-3}) observations in the soil profile (Ahuja and Lehman, 1983). Grey cells show cases where the model does not pass the fitness statistical test for α=0.1 (Ritter and Muñoz-Carpena, 2013). Numbers in squared brackets are 95% confidence interval. NSE and KGE are the Nash-Sutcliffe and Kling-Gupta Efficiency coefficients, respectively. RMSE is the model root mean square error, and p(NSE<0.5) or p(NSE<0.65) are the p-values for those selected minimum NSE thresholds. Symbols for cases are: C, L, SL: Ahuja and Lehman clay, loam and sandy loam soils; HL: Havis's loamy soil, p_h is for the optimized soil and transport parameters with Higashino-pumping boundary condition, np_h uses the same soil and transport parameters with no-pumping, np_c is the Hydrus 1-D no-pumping with optimization algorithm . Bias is considered negligible and not shown when <5%. Metrics for C, L and SL cases are calculated with observation uncertainties. Metrics for HL case are calculated without uncertainty.

Case	NSE [95% CI]	KGE [95% CI]	RMSE [95% CI]	p(NSE<0.65)	p(NSE<0.5)	% Bias
C_p_h	0.621 [0.242 - 0.893]	0.453 [0.101 - 0.747]	5.19x10^{-4} [2.71 x10^{-4} – 7.50x10^{-4}]	0.57	0.21	–
C_np_h	0.288 [-1.455 - 0.738]	0.403 [0. - 0.704]	7.10x10^{-4} [4.53x10^{-4} - 1.03x10^{-3}]	0.80	0.72	–
C_np_c	0.438 [-2.061 - 0.871]	0.510 [0.083 - 0.815]	6.31x10^{-4} [3.21 x10^{-4} - 1.06x10^{-3}]	0.70	0.52	–
L_p_h	0.977 [0.888 - 0.998]	0.891 [0.702 - 0.990]	2.10x10-4 [1.10x10-4 - 3.61x10-4]	0.00	0.00	–
L_np_h	0.886 [0.319 - 0.998]	0.799 [-0.068 - 0.982]	4.71x10-4 [1.24x10-4 - 8.82x10-4]	0.2	0.06	8.1
L_np_c	0.859 [0.145 - 0.994]	0.754 [-0.189 - 0.921]	5.23x10^{-4} [1.80x10^{-4} – 9.24x10^{-4}]	0.16	0.09	10.4
SL_p_h	0.997 [0.993 - 0.999]	0.915 [0.879 - 0.947]	5.46x10^{-5} [2.09x10^{-5} – 9.89x10^{-5}]	0.00	0.00	–
SL_np_h	0.997 [0.992 - 0.999]	0.876 [0.821 - 0.915]	6.32x10^{-5} [1.90x10^{-5} – 1.07x10^{-4}]	0.00	0.00	–
SL_np_c	0.938 [0.744 - 1.000]	0.836 [0.594 - 0.952]	2.70x10^{-4} [2.11x10^{-5} - 4.35x10^{-4}]	0.01	0.00	6.5
HL_p_h	0.881 [0.512 - 0.982]	0.822 [0.538- 0.946]	4.01x10^{-4} [2.23 x10^{-4}- 6.00 x10^{-4}]	0.071	0.02	
HL_np_h	0.077 [-1.094 - 0.826]	0.165 [-0.408 - 0.630]	1.12x10^{-3} [5.67 x10^{-4} - 1.55 x10^{-3}]	0.93	0.86	28.1

https://doi.org/10.5194/egusphere-2026-3253
Preprint. Discussion started: 24 June 2026

3.2. Depth of removal and mass of solute extracted

The depth of solute extraction (Figure 3 left, Table 3) was accurately predicted for all soils and experiments with the pumping boundary condition (p_h) with an average error of 2.8% across all soils, compared to -45% and and -48% for np_h and np_c, respectively. Interestingly, for the Ahuja and Lehman experiments and a rainfall intensity of 68 mm h^{-1}, deeper extraction was observed for the clay soil to a depth of -3.40 cm, followed by the loam with a depth of -2.46 cm and the sandy loam with a depth of -1.54 cm. For Havis loamy soil experiment with a rainfall intensity of 150 mm h^{-1}, an extraction depth of 2.79 cm was observed and was well simulated with the pumping boundary condition. This depth is larger than the depth of removal simulated for the loam experiment of Ahuja and Lehman, confirming that the rainfall intensity is also a factor influencing the depth of extraction. For Ahuja and Lehman's clay and loamy soils, the no-pumping boundary conditions (np_h and np_c) failed to capture the deeper extraction observed.

The closest prediction (within the experimental ranges of mass estimated) of mass removed from the clay and loamy soils was obtained with the pumping boundary condition (p_h) (Figure 3 right, Table 4). The no-pumping scenarios (np_h and np_c) largely underestimated the mass removed compared to the experimental mass. These results are consistent with the differences between the observed and predicted final concentration profiles (Figure 3). Based on the concentration profiles, as discussed above, the no-pumping scenarios did not reproduce the actual spatial dynamics of removal and extract more solute at shallow depths but do not extract as much solute deeper in the soil. For the sandy loam, the largest mass removal was simulated in the np_h scenario, but the mass from p_h was very close. The mass removed fell within the experimental range of mass estimated from the soil profile data for all scenarios except np_c. In the Havis simulations, the pumping scenario (p_h) predicted the mass removed very accurately, while the no-pumping scenario np_h largely underestimated the mass removed.

Table 3. Depth of solute extraction (cm), determined from soil concentration profiles observed by Ahuja and Lehman (1983) and Havis (1986) and predicted by the different simulations. Symbols for cases are p_h is for the optimized soil and transport parameters with Higashino-pumping boundary condition, np_h uses the same soil and transport parameters with no-pumping, np_c is the Hydrus 1-D no-pumping with optimization algorithm. Values in parenthesis are prediction error against the observed value.

.

Soil	Observation	p_h	np_h	np_c
C	-3.36	-3.40 (1%)	-1.34 (-60%)	-1.32 (-61%)
L	-2.30	-2.46 (7%)	-1.16 (-50%)	-1.08 (-53%)
SL	-1.50	-1.54 (3%)	-1.52 (1%)	-1.06 (-29%)
HL	-2.79	-2.79 (0%)	-0.80 (-71%)	-

https://doi.org/10.5194/egusphere-2026-3253
Preprint. Discussion started: 24 June 2026

Table 4. Mass removed from the soil per unit area (g cm^{-2}), determined from soil concentration profiles from Ahuja and Lehman (1983) and predicted by the different simulations, based on the final concentration profile in the soil. p_h is for the optimized soil and transport parameters with Higashino-pumping boundary condition, np_h uses the same soil and transport parameters with no-pumping, np_c is the Hydrus 1-D no-pumping with optimization algorithm. Grey cells indicate prediction outside the observation range.

Soil	Observation	p_h	np_h	np_c
C	0.00159 [0.00119-0.00199]	0.00121	0.00075 [0.00065-0.00081]	0.00065
L	0.00144 [0.00009 - 0.00279]	0.00106	0.00070 [0.00054-0.00071]	0.00061
SL	0.00087 [0.00063-0.00112]	0.0008	0.00085 [0.00067-0.00092]	0.0005
HL	0.00166	0.00169	0.00049	-

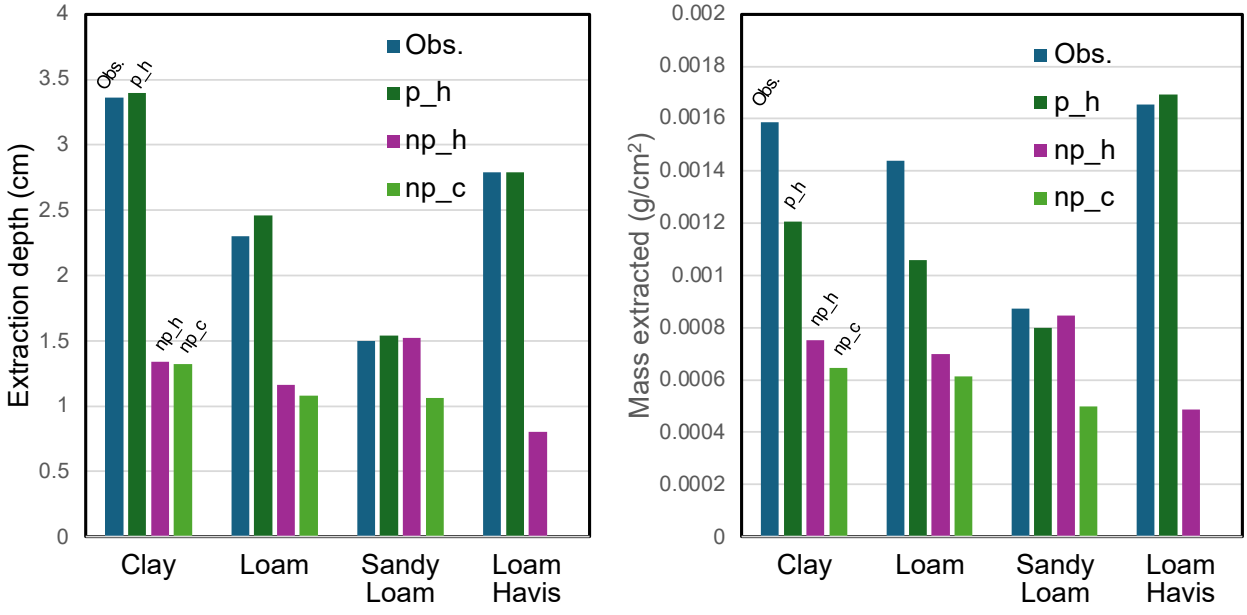

Figure 3. Comparison of simulated depth of removal and extracted mass against experimental data (Ahuja and Lehman, 1983, Havis, 1986). The mass extracted shown is obtained by integration of the soil concentration profile.

3.3. Physical consistency of the effective parameter values for the pumping scenario

For Ahuja and Lehman experiments, the effective runoff depths (d) for the pumping formulation in the clay and loamy soils was 0.052 cm, corresponding to the lower end of the initial range and close to the depth of 0.07 cm estimated by Wallach et

https://doi.org/10.5194/egusphere-2026-3253
Preprint. Discussion started: 24 June 2026

al. (1988) for these experiments using open channel flow equations. In the Higashino and Stefan (2014) formulation, the amplitude of the pumping wave h_o is inversely proportional to d (Eq. 2). Therefore, the small d for the clay and loamy soils resulted in a large h_o of 7.82 cm compared to the sandy loam soil where the effective d was 0.72 cm and h_o was 0.56 cm (Table 5). In Havis loam experiment with the large rainfall intensity, the resulting h_o was 16.7 cm.

Representative pressure values for the experiments of Ahuja and Lehman and Havis were identified from the response surface graphs (Figure 4) created from the experiments of Palmer (1965) and Yu and Hopkins (2018) and compared to the pressure heads simulated by the pumping boundary condition. For the clay and loam experiments of Ahuja and Lehman, the experimental range of pressure values derived from Figure 4 is 1.6 cm to 11.8 cm. The maximum pressure head simulated by the pumping boundary condition was 7.9 cm and falls inside this experimental range. For the sandy loam experiment of Ahuja and Lehman, the experimental range of pressure is 1.6 cm to 18.8 cm and the maximum simulated pressure head was 1.28 cm, which is close to that experimental range. For the loam experiment of Havis, the experimental range of pressure is 1.6 cm to 18.8 cm and the maximum simulated pressure head was 16.7 cm, which falls also inside the experimental range. These results confirm that the effective h_o values identified by the p_h model are physically consistent with those obtained independently for equivalent rainfall conditions by Palmer (1965) and Yu and Hopkins (2018).

https://doi.org/10.5194/egusphere-2026-3253
Preprint. Discussion started: 24 June 2026

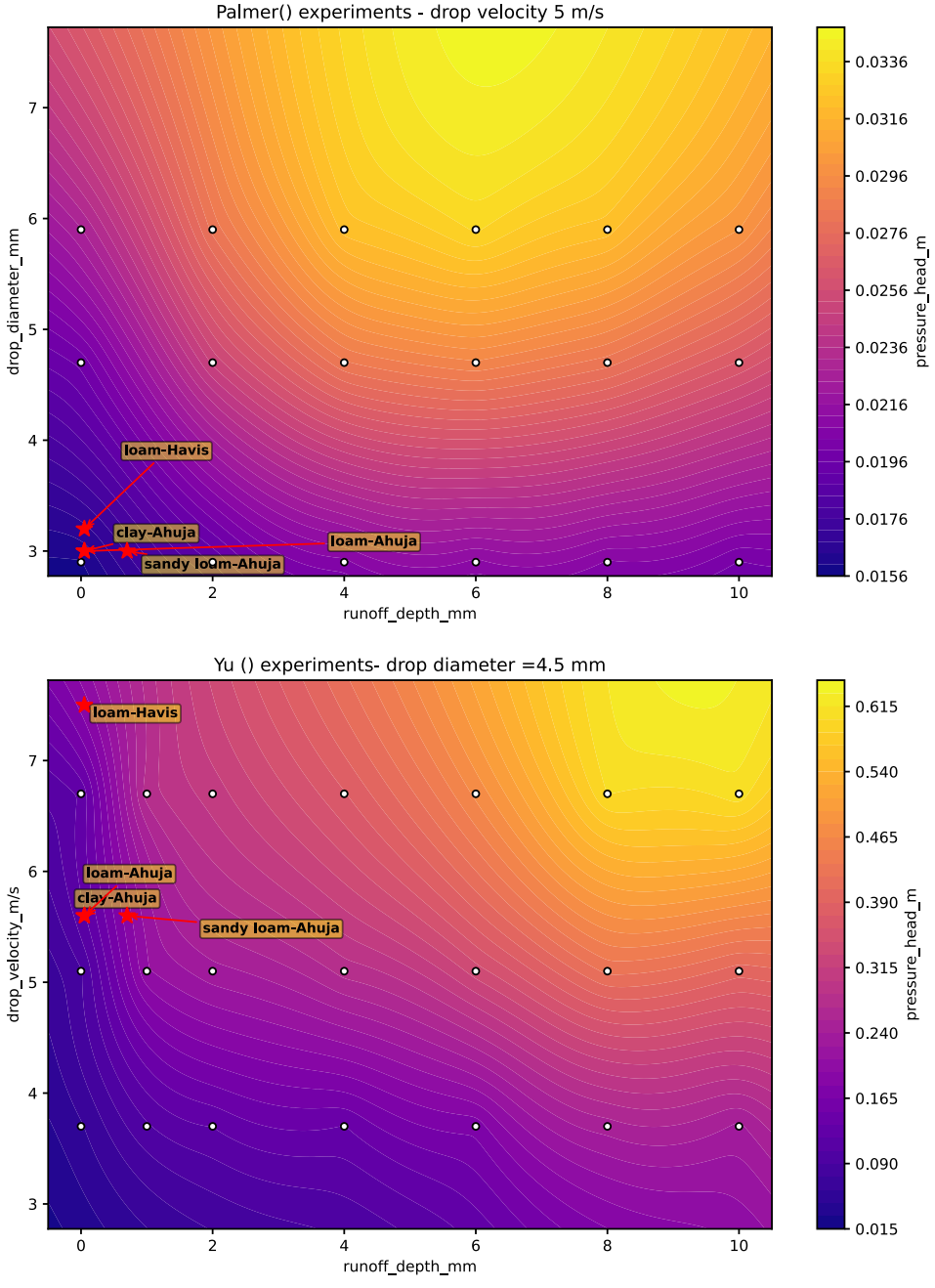

Figure 4. Surface response graphs created from Palmer (1965) and Yu and Hopkins (2018), with symbols indicating the experimental conditions of Ahuja and Lehman, (1983) and Havis (1986).

385 In the Higashino and Stefan (2014) formulation (Eq. 7), the frequency of the pumping wave ω_h is a function of the rainfall intensity only, so the same value of 6.48 s^{-1} was used for all three soils from Ahuja and Lehman (1983) for scenarios using this boundary condition (Table 5).

https://doi.org/10.5194/egusphere-2026-3253
Preprint. Discussion started: 24 June 2026

The lower n values of the clay and loamy soils are consistent with the wide distribution of pore sizes expected for these soils, compared to larger n value for sandy loam representing more homogeneous and larger pore sizes (Table 5). In the clay and loam pumping scenarios (C_p_h and L_p_h) the residual water contents θ_r were small and the inverse of the air entry pressure α was large compared to the sandy loam (SL_p_h) (Table 5). Low θ_r indicate that the clay and loam soils release most of the pore water when subjected to higher suction forces, and large α values indicate that these soils easily release water after saturation. Combined with the low runoff depths d that produce negative $h_{top,p}$ these conditions drive larger upward fluxes at the top of the soil for the clay and loam scenarios. This is consistent with the deeper solute extraction from the soil profile observed and modeled for the clay and loamy soils compared to the sandy loam. In the np_c scenarios, although all the parameters in Table 5 were selected for optimization, the Hydrus tool only changed the saturated hydraulic conductivity K_{sat} and the dispersivity λ (Table 5). In theory, the soil is in hydrostatic conditions with no water flow in this scenario because the soil is saturated, there is no bottom drainage, and the top boundary condition is a constant ponding depth. Therefore, the soil hydraulic parameters cannot be readily optimized.

Table 5. Effective parameters for Ahuja and Lehman (1983) and Havis (1986) modeling scenarios. θ_s is fixed as provided in Ahuja and Lehman (1983).

Type	Inputs	Pumping (p_h), no-pumping (np_h)				Hydrus classic (np_c)		
		C	L	SL	HL	C	L	SL
Soil hydraulic	vG θ_s(cm^3cm^{-3})	0.55	0.49	0.53	0.49	0.55	0.49	0.53
	vG θ_r (cm^3cm^{-3})	0.012	0.026	0.076	0.026	0.068	0.078	0.065
	vG α (cm^{-1})	0.119	0.176	0.030	0.176	0.008	0.036	0.075
	vG n	0.899	0.873	2.422	0.873	1.09	1.56	1.89
	vG K_{sat} (cm s^{-1})	0.0144	0.0340	0.0319	0.0340	$1.7x10^{-5}$	$2.9x10^{-4}$	$1.7x10^{-5}$
Transport	λ (cm)	956	274	495	274	10	1000	10
Effective runoff depth	d (cm)	0.052	0.052	0.720	0.052	-	-	-
Pumping amplitude	h_0 (cm) (Eq. 2)	7.82	7.82	0.56	16.73	-	-	-
Pumping frequency	ω_h (s^{-1}) (Eq. 7)	6.48	6.48	6.48	1.24	-	-	-
Top pressure head	$h_{top,p}$ (cm) (Eq. 1)	[-7.77,7.87]	[-7.77,7.87]	[0.16,1.28]	[-16.7,16.8]	-	-	-

https://doi.org/10.5194/egusphere-2026-3253
Preprint. Discussion started: 24 June 2026

3.4. Global sensitivity analysis: importance of rainfall pumping input factors

The sensitivity of the mass removed from the soil to the model inputs was analyzed for the pumping scenario (p_h). For all soils, the sum of the first order sensitivity indexes $\sum S_i$ was above 0.6 for an additive model, indicating that the variance in the predicted mass removed from the soil is mainly explained by the individual contributions (direct effects) of the input parameters (Table 6). The only input factor of first order importance is d, which explains 69 to 72 % of the variance. According to Eq. 2, d controls the magnitude of the variable pressure head (h_o) and flux caused by the rainfall pumping, and therefore the mass removal.

The van Genuchten α and n input factors exhibited second order importance with $S_{Ti} \approx$16% and 20%, respectively, which is significantly larger than their first-order indices of < 2 and 5 %, respectively. This indicates that these input factors influence the model output through interactions with other factors such as d. In this saturated modeling scenario, the pumping boundary condition forces surface pores to alternately drain and refill. As noted earlier, the inverse of the air-entry pressure, α represents the suction at which the soil starts to desaturate and water is released. The input n represents the pore-size distribution, which governs the hydraulic conductivity near saturation and therefore the magnitude of the flux at the surface. Because these parameters determine the soil's responsiveness to changes in pressure oscillations, their impact is only significant when the soil is subjected to a pumping boundary condition.

The other inputs had less than 5% contributions by themselves or with interactions indicating that for the conditions of the experimental problem and modeling representation studied here they were unimportant to explain the mass extracted from the soil. The model exhibits low sensitivity to saturated hydraulic conductivity K_{sat} because the system is fully saturated and does not have bottom drainage. In the absence of a large hydraulic gradient, conductivity parameters do not influence the simulation outcomes

https://doi.org/10.5194/egusphere-2026-3253
Preprint. Discussion started: 24 June 2026

Table 6. Sobol's global sensitivity analysis variance decomposition by pumping scenario for mass removed from soil (g cm^{-2}) model output. S_i and S_{Ti} are first order and total order sensitivity indices; C, L, SL are soil types: clay, loam and sandy loam; $\sum S_i$ is the sum of the first order S_i. Cells in grey represent inputs with contributions to the output variance >5%. Input ranges for the analysis are provided in Table 1.

	Higashino					
Inputs	C_p_h		L_p_h		SL_p_h	
	S_i	S_{Ti}	S_i	S_{Ti}	S_i	S_{Ti}
d	0.686	0.983	0.692	0.997	0.716	1.010
λ	0.003	0.011	0.003	0.010	0.003	0.010
vG θ_r	0.003	0.003	0.003	0.021	0.003	0.003
vG α	0.017	0.168	0.020	0.146	0.018	0.169
vG n	0.047	0.206	0.047	0.213	0.046	0.204
vG K_{sat}	0.002	0.078	0.008	0.069	0.005	0.073
$\sum S_i$	0.758	--	0.773	--	0.791	--

4. Discussion

The results demonstrate that the rainfall pumping boundary condition based on Higashino and Stefan (2014) formulation (p_h) combined with Richards soil flow and advection dispersion transport equations consistently outperforms conventional no-pumping boundary conditions (np_h and np_c) across all tested soil textures. The most critical improvements were observed in the finer-textured soils, specifically clay and loam.

A key strength of the pumping boundary condition is its ability to adequately predict the vertical dynamics of solute removal and redistribution in the soil during the rainfall events, compared to the no-pumping boundary conditions. As a result, the pumping boundary condition accurately predicts the depth of solute extraction and mass extracted that vary significantly by soil type, with the clay soil experiencing deeper extraction, followed by the loam and the sandy loam for a given rainfall intensity. The no-pumping boundary conditions failed to capture these deeper and larger extraction patterns in clay and loam. For the sandy loam, the pumping boundary condition was only marginally better than the classical boundary condition, suggesting that the added value of the mechanistic pumping approach is less pronounced in coarse soils.

https://doi.org/10.5194/egusphere-2026-3253
Preprint. Discussion started: 24 June 2026

The robustness of the mechanistic pumping boundary condition is further evidenced by its performance when applied to the independent dataset from Havis (1986) on loamy soil, which used a larger rainfall intensity (150 mm h^{-1} vs. 68 mm h^{-1}). In this simulation, the loamy soil parameters calibrated from the Ahuja and Lehman data were directly applied without further adjustment. By correctly scaling the pumping amplitude as a function of the increased rainfall intensity (h_0=16.7 cm), the model successfully captured the enhanced advective transport observed during that high-intensity experiment. The pumping boundary condition (HL_p_h) maintained higher accuracy over the no-pumping approach (HL_np_h) confirming that it accurately captured the processes of solute remobilization across varying rainfall intensities and soil types.

Previous attempts to model the experimental data from Ahuja and Lehman (1983) have employed different strategies with notable limitations. A significant drawback of these previous works is the lack of quantified goodness-of-fit indicators, which prevents a direct, objective comparison of model performance. Wallach et al. (1988) used an enhanced mass transfer process but only presented results for the loam experiment, for which findings from this study suggest nearly any boundary condition provides acceptable results. Other studies (Walter et al., 2007; Zhang et al., 1999) utilized a "mixing layer" approach, where a layer of fixed depth releases solute to runoff and interacts with the underlying soil via diffusion. These studies failed to reproduce the experimental final soil concentration profiles. Their simulations typically show that the top of the soil profile, corresponding to the “mixing layer” is almost completely depleted of solute, which contradicts the observed data where the finer clay soil experienced deeper extraction. In contrast, the pumping boundary condition proposed in our study provides a robust mechanistic framework that accurately captures the deeper redistribution of solutes.

While the pumping boundary condition outperformed the no-pumping boundary condition, it is important to acknowledge some limitations in this study. In the Ahuja and Lehman (1983) experimental datasets, there was substantial variability in the soil solute data between replicated experiments. This indicates that the initial distribution of bromide in the soil may not have been uniform with depth and varied between replicates. Furthermore, for the clay and loamy soils, the final measured concentration at depths below 2.5 cm exceeded the initial concentration value reported in the original article, suggesting that the initial concentrations may have been larger than stated. This limitation was addressed in our study by propagating the uncertainty on this initial condition through the model. In addition, while the pumping model achieved adequate and the best fit for clay (NSE = 0.620), its overall performance for this soil was lower than for loam or sandy loam. Ahuja and Lehman (1983) reported that the Parsons clay soil exhibited some swelling upon wetting, which could have altered its intended bulk density and porosity during the experiments. Such changes in physical properties are not accounted for in our model and may contribute to the lesser model performance observed for the clay soil compared to the other soils. The experiment from Havis (1986) was not replicated and also exhibited scatter in the final soil concentrations. Finally, this study uncovers the need and opportunities to further refine the rainfall pumping formulation proposed by Higashino and Stefan (2014). In this formulation the amplitude term is inversely proportional to the runoff depth (Eq. 2), where the experimental data from Palmer (1965) and Yu and Hopkins (2018) suggests that the relationship between runoff depth and pressure head is more complex (Figure 4).

https://doi.org/10.5194/egusphere-2026-3253
Preprint. Discussion started: 24 June 2026

5. Conclusions

This study successfully demonstrated that a mechanistic modeling approach coupling a "rainfall pumping" boundary condition to classical soil flow and transport equations significantly improves the simulation of solute remobilization from soil to runoff compared to a classical diffusion-only boundary condition. This study represents the first application of a rainfall pumping boundary condition to two independent experimental datasets (the widely-cited Ahuja and Lehman, 1983 and Havis, 1986), corrects a key error in the original pumping formulation by Higashino and Stefan (2014), and evaluates the robustness of the proposed modeling approach across soil types and rainfall intensities.

The proposed modeling approach provides accurate estimations of key solute remobilization outputs, including the final soil concentration profiles, the depth of solute extraction, and the total mass of solute extracted from the soil. The superior performance of the pumping boundary condition over the conventional boundary condition, especially on fine soils, highlights the contribution of advective transport to chemical removal from soils subjected to pumping events.

This work demonstrates that more comprehensive experimental datasets are needed to further validate the rainfall pumping approach and evaluate its application to realistic conditions. Future laboratory studies should focus on measuring solute concentrations in the soil at higher spatial resolutions to better capture the depth of extraction and the mass of solute extracted, as well as measurement of solute concentrations in the runoff to close the solute mass balance. In addition, future experiments should investigate a broader range of soil types and properties, rainfall intensities, raindrop characteristics, and runoff depths to identify the experimental factors that control solute extraction. Experiments on unsaturated soils with downward leaching and sorbed chemicals are also required to extend the proposed modeling approach to more realistic conditions.

Future work is also needed to reduce the semi-empiricism in the pumping boundary condition formulation in favor of more physically-based formulations that reduce the need for calibration. Another refinement would be to include an explicit coupling between the soil domain and the runoff domain, as done in Wallach et al. (2001) but considering the rainfall pumping to improve the solute boundary condition at the soil runoff interface.

Advancing the mechanistic modeling of solute remobilization from soil to runoff during a rainfall event will critically enhance our ability to accurately predict contaminant transport across a wide range of applications, including design, environmental risk assessments, and management.

Code and data availability

The scripts and data used in the paper are shared in a public repository at https://github.com/carpena1/pumping_repository

https://doi.org/10.5194/egusphere-2026-3253
Preprint. Discussion started: 24 June 2026

Author contributions

Conceptualization: LG and RMC, Data Curation: LG, Investigation, Methodology, and Formal Analysis; LG and RMC, Resources: RMC, Visualization; LG and RMC, Writing (original draft preparation): LG and RMC. Writing (review and editing): LG and RMC.

Acknowledgements

The authors acknowledge University of Florida IT Research Computing for providing computational resources and support that have contributed to the research results reported in this publication. URL: http://www.rc.ufl.edu.

Financial Support

RMC acknowledges the support received by the Hatch Multistate Research projects S1089 and W5045 from the U.S. Department of Agriculture's National Institute of Food and Agriculture.

References

Ahuja, L. R., and Lehman, O. R.: The extent and nature of rainfall-soil interaction in the release of soluble chemicals to runoff, J. Environ. Qual., 12, 34–40, https://doi.org/10.2134/jeq1983.00472425001200010005x, 1983.

Beven, K. J., Ed Henderson, D., and Reeves, A. D.: Dispersion parameters for undisturbed partially saturated soil, J. Hydrol., 143, 19–43, https://doi.org/10.1016/0022-1694(93)90087-P, 1993.

Bruce, R. R., Harper, L. A., Leonard, R. A., Snyder, W. M., and Thomas, A. W.: A Model for Runoff of Pesticides from Small Upland Watersheds, J. Environ. Qual., 4, 541–548, https://doi.org/10.2134/jeq1975.00472425000400040024x, 1975.

Deng, L., Fei, K., Sun, T., Zhang, L., Fan, X., and Ni, L.: Characteristics of runoff processes and nitrogen loss via surface flow and interflow from weathered granite slopes of Southeast China, J. Mt. Sci., 16, 1048–1064, https://doi.org/10.1007/s11629-018-5253-2, 2019.

Gupta, H. V., Kling, H., Yilmaz, K. K., and Martinez, G. F.: Decomposition of the mean squared error and NSE performance criteria: Implications for improving hydrological modelling, J. Hydrol., 377, 80–91, https://doi.org/10.1016/j.jhydrol.2009.08.003, 2009.

Havis R. N., Solute transport from soil to overland flow. PhD Dissertation Colorado State University, 1986.

Havis, R. N., Smith, R. E., and Adrian, D. D.: Partitioning solute transport between infiltration and overland flow under rainfall, Water Resour. Res., 28, 2569–2580, https://doi.org/10.1029/92WR01366, 1992.

Haynes, W. M. (Ed.): CRC Handbook of Chemistry and Physics (97th ed.), CRC Press, https://doi.org/10.1201/9781315380476, 2016.

https://doi.org/10.5194/egusphere-2026-3253
Preprint. Discussion started: 24 June 2026

Herman, J., and Usher, W.: SALib: An open-source Python library for Sensitivity Analysis, J. Open Source Softw., 2, 97, https://doi.org/10.21105/joss.00097, 2017.

Higashino, M., and Stefan, H. G.: Modeling the effect of rainfall intensity on soil-water nutrient exchange in flooded rice paddies and implications for nitrate fertilizer runoff to the Oita River in Japan, Water Resour. Res., 50, 8611–8624, https://doi.org/10.1002/2014WR015615, 2014.

Lauvernet, C., and Muñoz-Carpena, R.: Shallow water table effects on water, sediment, and pesticide transport in vegetative filter strips – Part 2: Model coupling, application, factor importance, and uncertainty, Hydrol. Earth Syst. Sci., 22, 71–87, https://doi.org/10.5194/hess-22-71-2018, 2018.

Luquin, E., Campo-Bescós, M. A., Muñoz-Carpena, R., Bingner, R. L., Cruse, R. M., Momm, H. G., Wells, R. R., and Casalí, J.: Model prediction capacity of ephemeral gully evolution in conservation tillage systems, Earth Surf. Proc. Land., 46, 1909–1925, https://doi.org/10.1002/esp.5134, 2021.

Meyer, P. D., and Taira, R. Y.: Hydrologic Uncertainty Assessment for Decommissioning Sites: Hypothetical Test Case Applications (NUREG/CR-6695, PNNL-13375), U.S. Nuclear Regulatory Commission, https://www.nrc.gov/reading-rm/doc-collections/nuregs/contract/cr6695/index, 2001.

Moriasi, D. N., Arnold, J. G., Van Liew, M. W., Bingner, R. L., Harmel, R. D., and Veith, T. L.: Model evaluation guidelines for systematic quantification of accuracy in watershed simulations, Trans. ASABE, 50, 885–900, 2007.

Nash, J. E., and Sutcliffe, J. V.: River flow forecasting through conceptual models part I — A discussion of principles, J. Hydrol., 10, 282–290, https://doi.org/10.1016/0022-1694(70)90255-6, 1970.

Palmer, R. S.: Waterdrop impact forces, Trans. ASAE, 8, 69–70, https://doi.org/10.13031/2013.40428, 1965.

Parr, A., Richardson, C., Lane, D., and Baughman, D.: Pore water uptake by agricultural runoff, J. Environ. Eng., 113, 49–63, 1987.

Ritter, A., and Muñoz-Carpena, R.: Performance evaluation of hydrological models: Statistical significance for reducing subjectivity in goodness-of-fit assessments, J. Hydrol., 480, 33–45, https://doi.org/10.1016/j.jhydrol.2012.12.004, 2013.

Saltelli, A.: Sensitivity Analysis for Importance Assessment, Risk Anal., 22, 579–590, https://doi.org/10.1111/0272-4332.00040, 2002.

Saltelli, A.: Global sensitivity analysis: An introduction, Proc. 4th International Conference on Sensitivity Analysis of Model Output (SAMO'04), 27, 43, 2004.

Saltelli, A., Ratto, M., Andres, T., Campolongo, F., Cariboni, J., Gatelli, D., Saisana, M., and Tarantola, S.: Global sensitivity analysis: The primer, John Wiley and Sons, 2008.

Saltelli, A., Ratto, M., Tarantola, S., and Campolongo, F.: Sensitivity Analysis for Chemical Models, Chem. Rev., 105, 2811–2828, https://doi.org/10.1021/cr040659d, 2005.

Shao, F., Tao, W., Wang, Q., Wu, J., Su, L., Sun, Y., and Zeng, S.: A modified model for predicting nutrient loss in runoff using a time-varying mixing layer, J. Hydrol., 603, 127091, https://doi.org/10.1016/j.jhydrol.2021.127091, 2021.

https://doi.org/10.5194/egusphere-2026-3253
Preprint. Discussion started: 24 June 2026

Šimůnek, J., Van Genuchten, M. Th., and Šejna, M.: Development and Applications of the HYDRUS and STANMOD Software Packages and Related Codes, Vadose Zone J., 7, 587–600, https://doi.org/10.2136/vzj2007.0077, 2008.

Snyder, J. K., and Woolhiser, D. A.: Effects of infiltration on chemical transport into overland flow, Trans. ASAE, 28, 1450–1457, 1985.

Sobol, I. M.: Sensitivity analysis for non-linear mathematical models, Math. Model. Comput. Exp., 1, 407–414, 1993.

Thompson, S. E., Katul, G. G., and Porporato, A.: Role of microtopography in rainfall-runoff partitioning: An analysis using idealized geometry, Water Resour. Res., 46, W07520, https://doi.org/10.1029/2009WR008835, 2010.

van Genuchten, M. Th.: A Closed-form Equation for Predicting the Hydraulic Conductivity of Unsaturated Soils, Soil Sci. Soc. Am. J., 44, 892–898, https://doi.org/10.2136/sssaj1980.03615995004400050002x, 1980.

Wallach, R., Jury, W. A., and Spencer, W. F.: Transfer of Chemicals from Soil solution to Surface Runoff: A Diffusion-based Soil Model, Soil Sci. Soc. Am. J., 52, 612–618, https://doi.org/10.2136/sssaj1988.03615995005200030002x, 1988.

Wallach, R., and Shabtai, R.: Surface runoff contamination by chemicals initially incorporated below the soil surface, Water Resour. Res., 29, 697–704, https://doi.org/10.1029/92WR02160, 1993.

Wallach, R., Grigorin, G., and Byk, J. R.: A comprehensive mathematical model for transport of soil-dissolved chemicals by overland flow, J. Hydrol., 247, 85–99, https://doi.org/10.1016/S0022-1694(01)00366-2, 2001.

Walter, M. T., Gao, B., and Parlange, J.-Y.: Modeling soil solute release into runoff with infiltration, J. Hydrol., 347, 430–437, https://doi.org/10.1016/j.jhydrol.2007.09.033, 2007.

Wang, Q., Horton, R., and Shao, M.: Effective Raindrop Kinetic Energy Influence on Soil Potassium Transport into Runoff, Soil Sci., 167, 369–376, https://doi.org/10.1097/00010694-200206000-00002, 2002.

Young, D. F., and Fry, M. M.: Field-scale evaluation of pesticide uptake into runoff using a mixing cell and a non-uniform uptake model, Environ. Modell. Softw., 122, 104055, https://doi.org/10.1016/j.envsoft.2017.09.007, 2017.

Yu, Y., and Hopkins, C.: Experimental determination of forces applied by liquid water drops at high drop velocities impacting a glass plate with and without a shallow water layer using wavelet deconvolution, Exp. Fluids, 59, 84, https://doi.org/10.1007/s00348-018-2536-1, 2018

Zhang, X., Norton, L., Lei, T., and Nearing, M.: Coupling mixing zone concept with convection-diffusion equation to predict chemical transfer to surface runoff, Trans. ASAE, 42, 987–994, 1999.

Zhang, Y., Zhang, X., Shi, S., Li, H., and Xiao, P.: Determining the depth of mixing layer in which soil solute releasing from soil to surface runoff on the unsaturated loess slope under artificial rainfall condition, J. Soils Sediments, 20, 153–165, https://doi.org/10.1007/s11368-019-02370-y, 2020.